a

***FoxA1* gene expression in normal tissues (GEO database):**

Mostly expressed in Prostate, Breast, Liver, Colon, Lung, Bladder, Stomach, Trachea

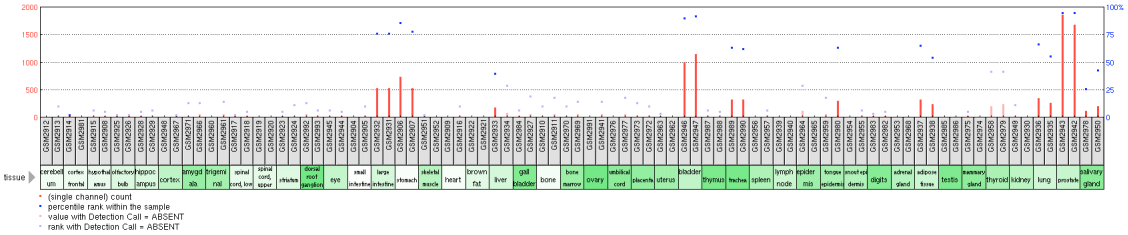

b

***FoxA1* gene expression in cancer cell lines (Gene Expression Atlas database):**

Highly expressed in Prostatic LNCaP, Breast MCF7, and Liver, Colon, & Lung Cancer cell lines

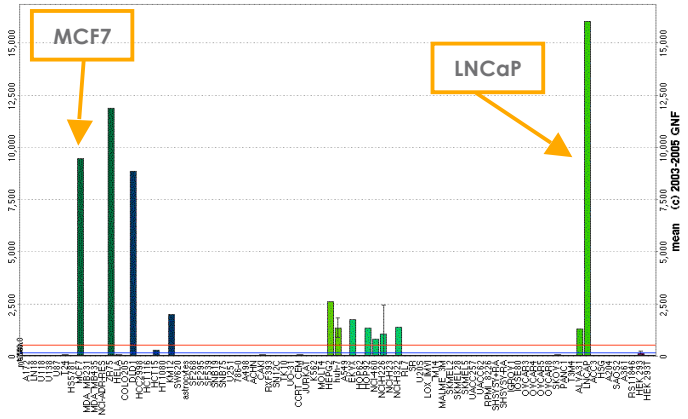

Supplementary Figure 1. Lineage-specific expression of FoxA1 in normal prostatic tissue and prostate cancer cells. (a) *FOXA1* tissue expression profile was extracted from the GEO database. **(b)** *FOXA1* cancer cell line expression profile was obtained from the Gene Expression Atlas database.

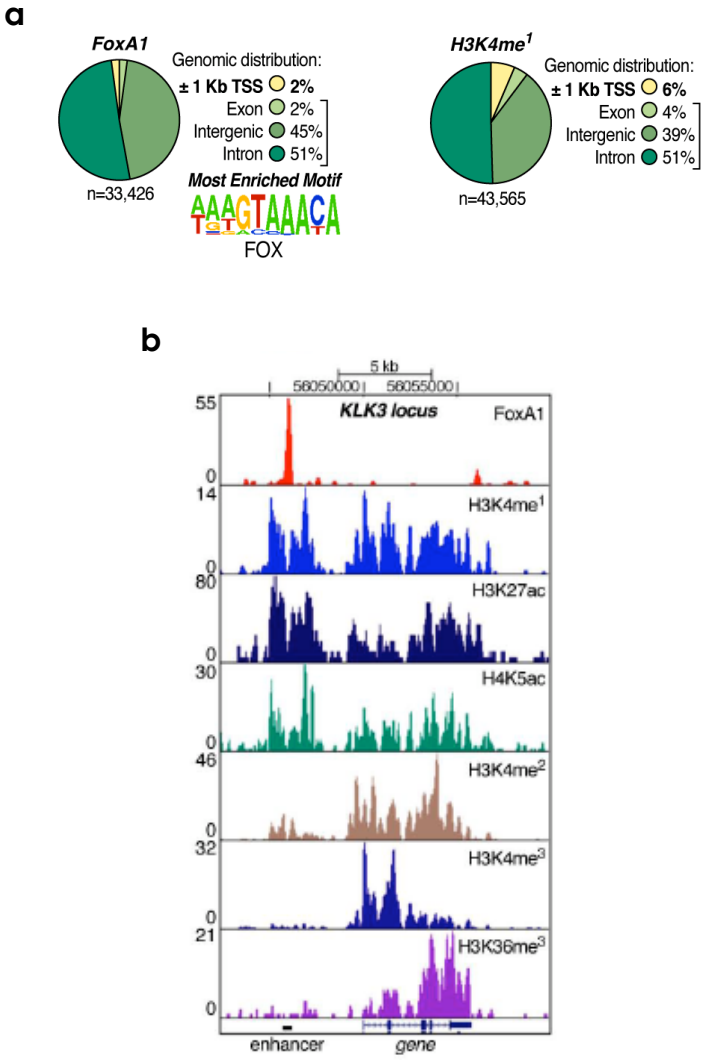

Supplementary Figure 2. FoxA1 binding and histone marks on the *KLK3* locus. (a) Genomic distribution of FoxA1 (n=33,426; left) and H3K4me1-positive, H3K4me3-negative (n=43,565; right) loci with respect to annotated genes. The most enriched motif on FoxA1 loci is the FOX binding site. (**b**) Shown are the distribution of FoxA1, H3K4me1, H3K27ac, H4K5ac, H3K4me2, H3K4me3, and H3K36me3 in DHT-treated LNCaP cells around the well-characterized androgen regulated *KLK3* gene. The y axe displays the number of normalized ChIP-seq tags. The position of the gene and the location of a reported upstream enhancer site are indicated at bottom.

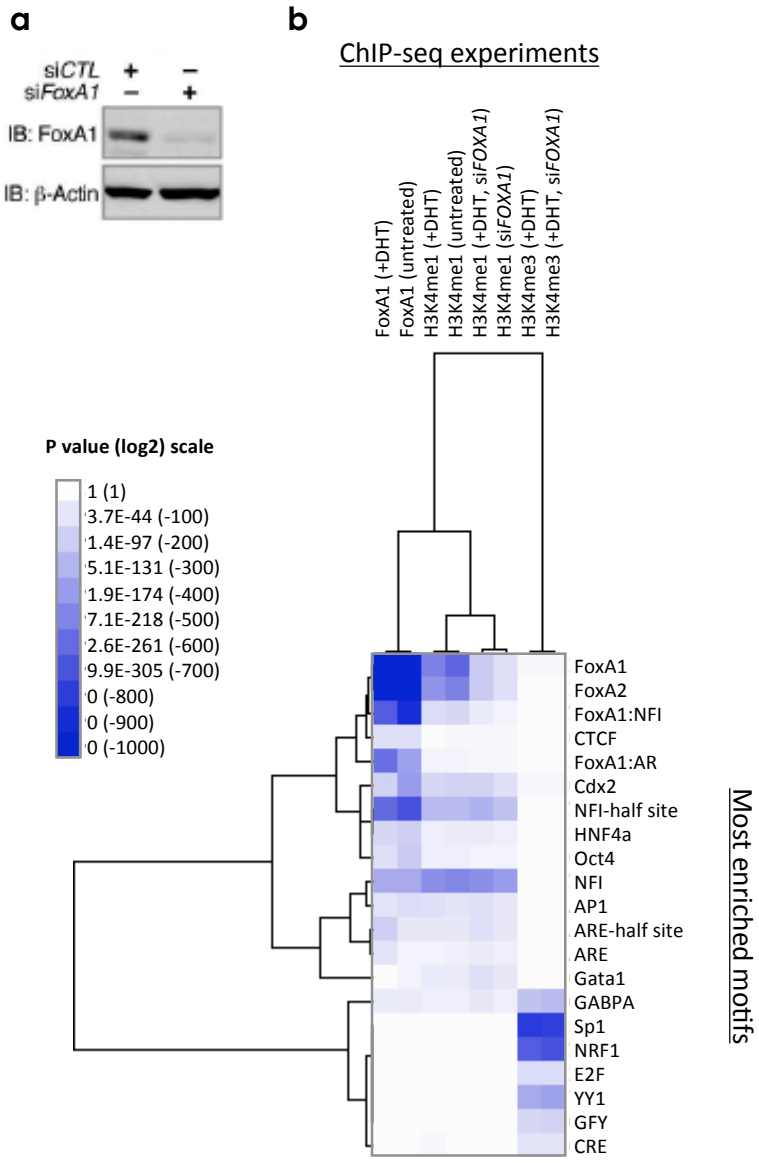

Supplementary Figure 3. FoxA1 is a major component on H3K4me1-marked regions in LNCaP cells. (a) Efficacy of *FOXA1* knockdown by siRNA. **(b)** Hierarchical clustering of motif enrichment in regions obtained by ChIP-seq of H3K4me1, H3K4me3, and FoxA1 demonstrates co-enrichment of the same FOX motif in H3K4me1 and FoxA1 loci. Enrichment of this same motif was selectively lost upon *FOXA1* siRNA treatment. Only motifs with a hypergeometric enrichment of at least 10^{-50} in at least one experiment were included.

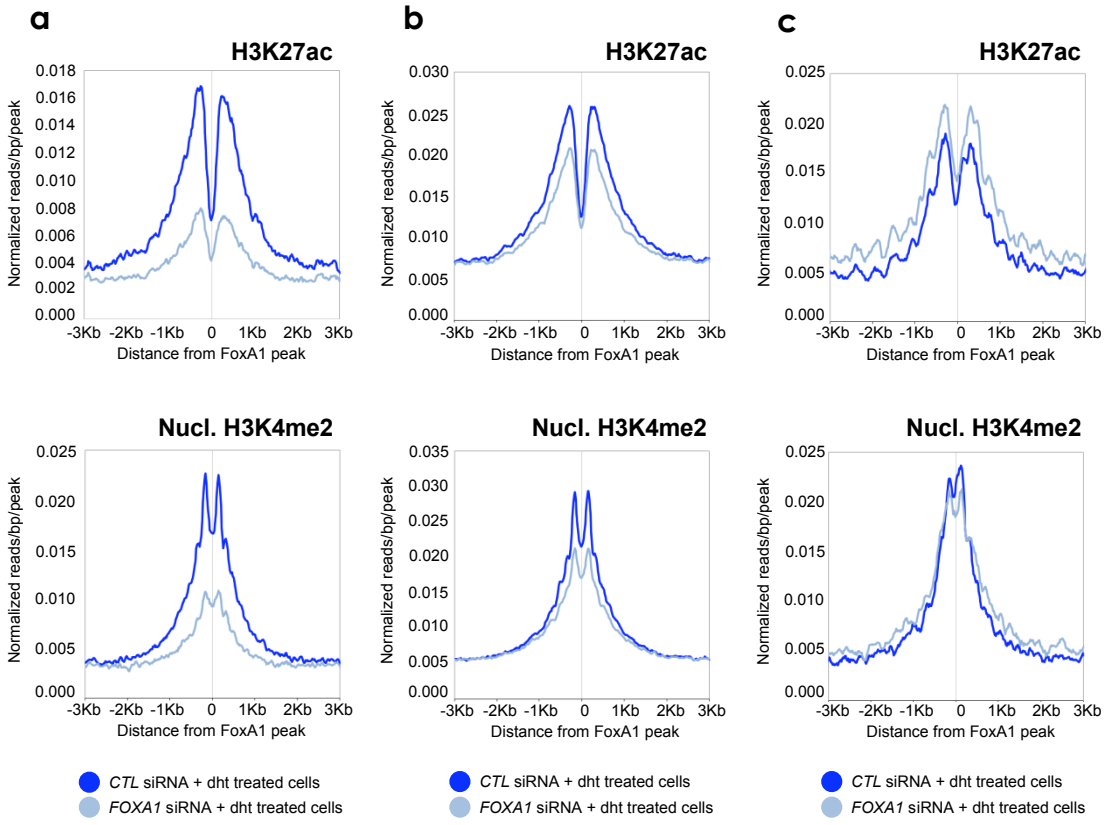

Supplementary Figure 4. Effect of *FOXA1* knockdown on H3K27ac and H3K4me2. Corresponding changes in H3K27ac (*top*) and H3K4me2 (*bottom*) marks around FoxA1-bound loci classified based on differential responses (a: decreased, b: no significant change, c: increase) of H3K4me1 to *FOXA1* knockdown (see Fig.1g-i). Profiles shown for H3K4me2 are at the nucleosomal resolution.

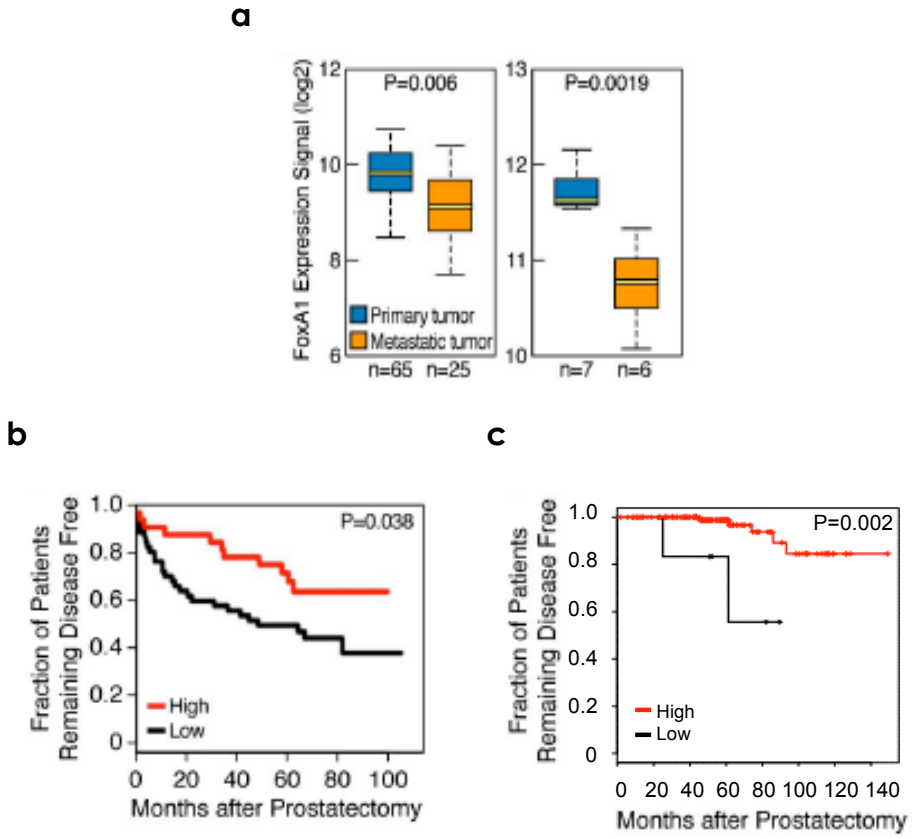

Supplementary Figure 5. FoxA1 downregulation is significantly associated with metastatic prostate cancer and poor prognosis. (a) *FOXA1* levels in primary and metastatic prostate tumors based on published gene expression profiling studies (left: GDS2545, ref. 36,37; right: GDS1439, ref. 38). **(b)** Kaplan-Meier plot of overall survival rates on a cohort of prostate cancer patients after prostatectomy (ref. 39). Patients are divided into two groups based on relative low (n=47; black) or high (n=31; red) *FOXA1* mRNA expression at the time of prostatectomy. *P*-value for the difference is indicated. **(c)** Kaplan-Meier plot of overall survival rates on another cohort of prostate cancer patients after prostatectomy (ref. 40). Patients were divided into two groups of based on relative low (n=7; black) or high (n=124; red) *FOXA1* mRNA expression at the time of prostatectomy. *P*-value for the difference is indicated.

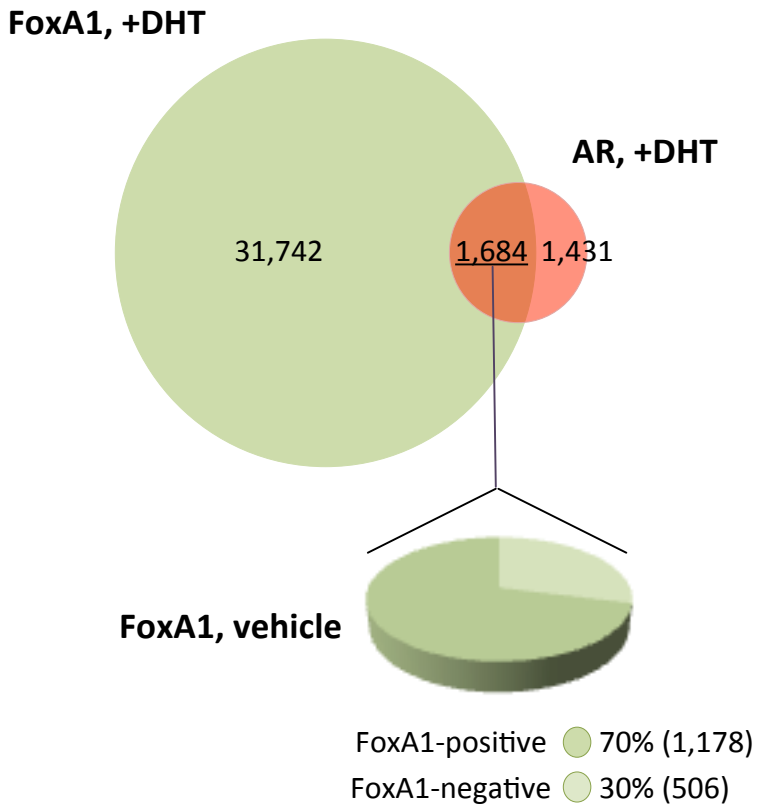

Supplementary Figure 6. Co-incidence of DHT-induced AR genomic loci with FoxA1 binding in LNCaP cells. Venn diagram of FoxA1 (n=33,426) and AR (n=3,115) bound loci detected by ChIP-seq in DHT-treated LNCaP cells at FDR<0.001. Among the overlapping sites, 70% is bound by FoxA1 before DHT treatment as indicated by the figure at the lower portion.

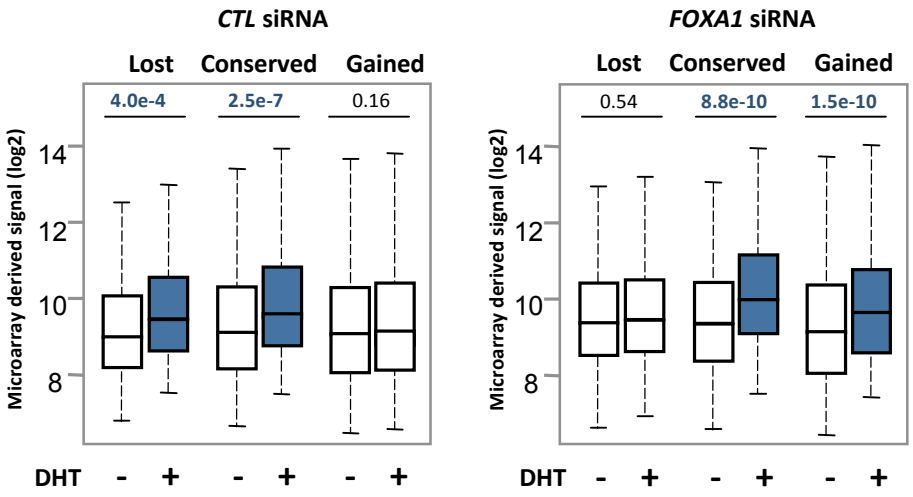

Supplementary Figure 7. Different effects of *FOXA1* knockdown on individual DHT-induced gene expression programs. The microarray expression data of up-regulated genes are compared in the lost, conserved, and gained programs before (-) and after (+) of DHT treatment in LNCaP cells that have been either mock-treated with control siRNA (left) or with *FOXA1* siRNA (right). Up-regulated groups are highlighted in filled boxed. Outliers were omitted from box plots. *P*-values are shown to highlight the significance in each case.

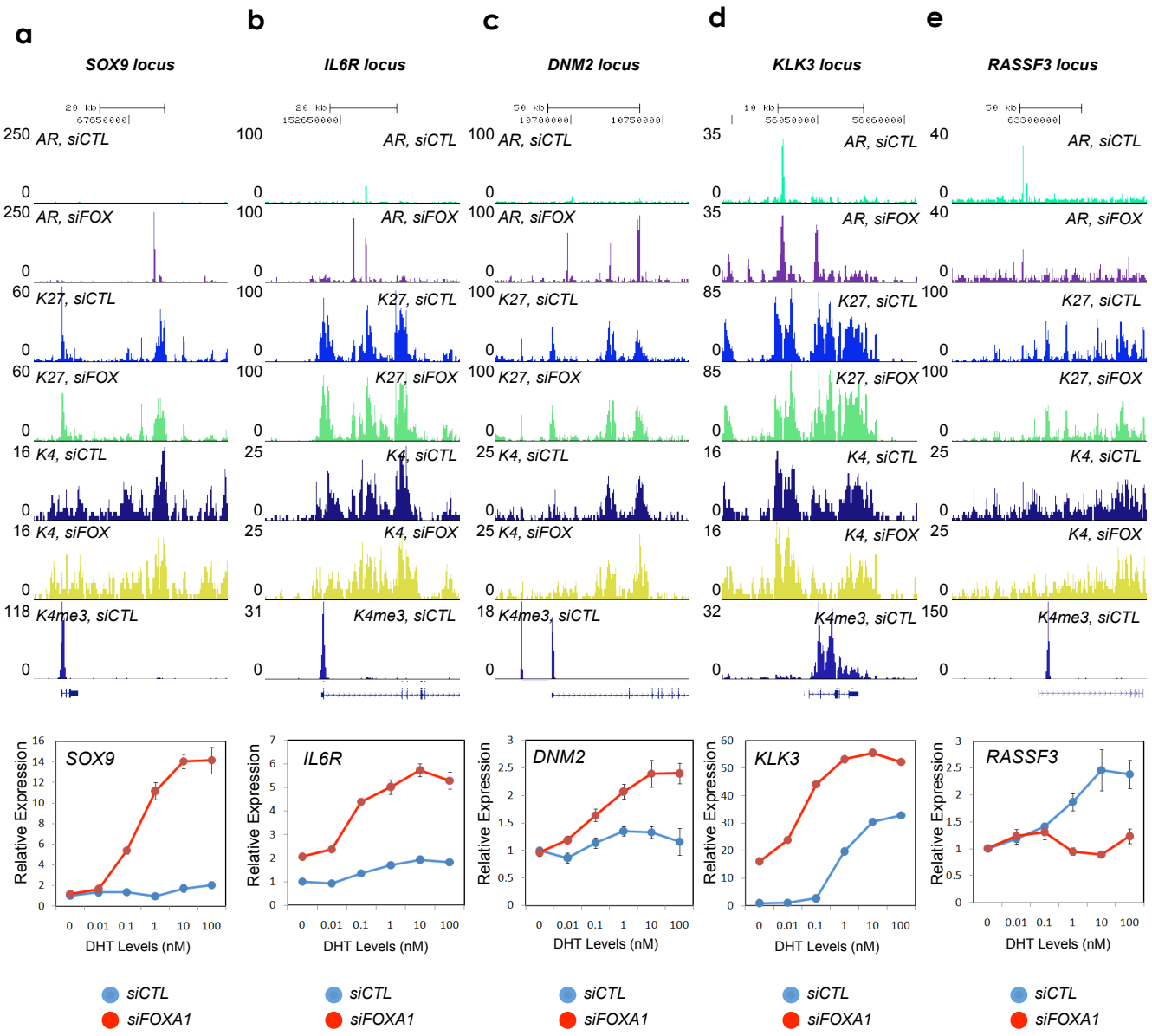

Supplementary Figure 8. Illustrative examples of AR reprogrammed genes. (a-c) Top panels: Examples of gained AR binding sites located within pre-existing epigenetic-marked, non-promoter regions. Shown are ChIP-seq profiles of AR, H3K27ac (K27), and H3K4me1 (K4) in control siRNA or *FOXA1* siRNA treated cells, and profile of H3K4me3 (K4me3) in control siRNA treated cells. Bottom panels: Responsiveness to increasing amounts of DHT in control siRNA or *FOXA1* siRNA treated cells, determined by RT-qPCR. **(d)** As example of AR binding (top) and gene expression (bottom) from the conserved program. **(e)** An example of AR binding site (top) and gene expression (bottom) in the lost program. Mean ±s.e.m. is based on three independent experiments.

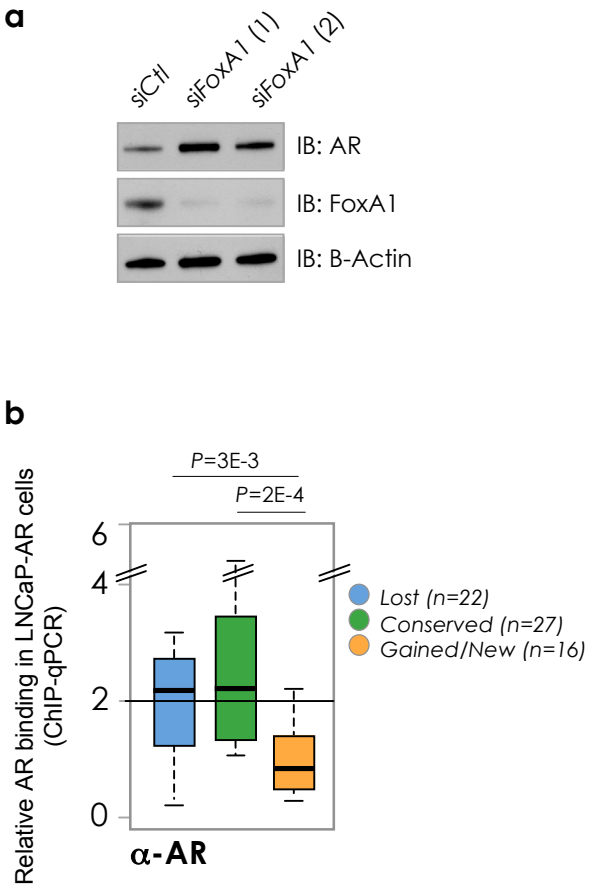

Supplementary Figure 9. Effect of AR overexpression on AR genomic binding. (a) Effect of *FOXA1* knockdown on AR protein. Two different *FOXA1* siRNAs tested (#1 and #2) induced AR. **(b)** Summary of ChIP-qPCR validated AR binding events on randomly selected genes from the lost (n=22), conserved (n=27), and gained (n=16) programs in LNCaP-AR cells, which is derived from LNCaP cells stably over-expressing AR. These genomic loci were the same tested for Fig. 2e. *P*-values show the significant differences detected.

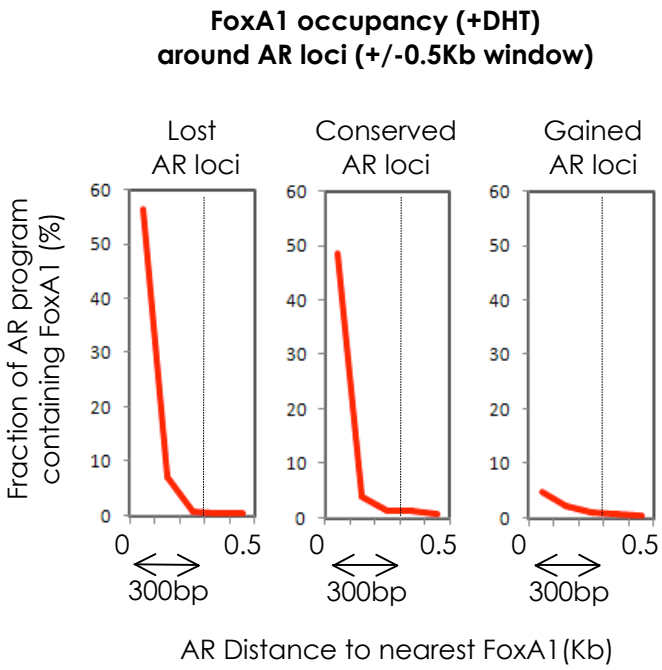

Supplementary Figure 10. Relative FoxA1 occupancy levels in the lost, conserved, and gained AR binding programs. The data show that FoxA1 binding is highly enriched in the vicinity (300bp) of AR binding sites in both the lost (62%) and conserved (52%) AR binding programs, but not in the gained AR binding program (7%).

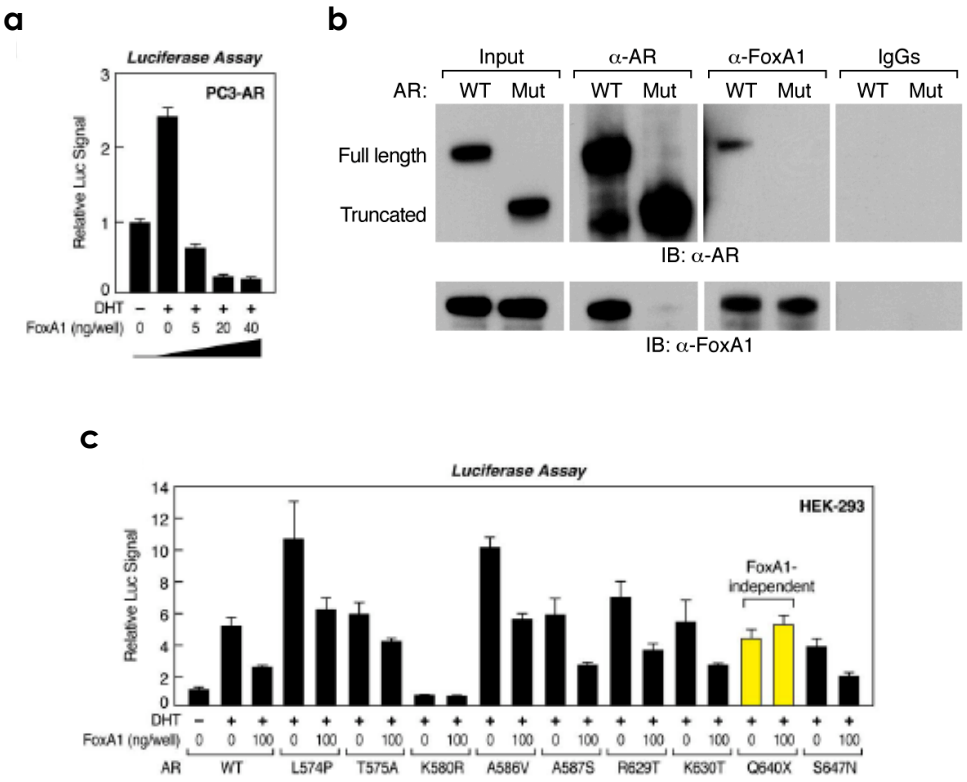

Supplementary Figure 11. FoxA1 squelches AR-dependent transcription from an ARE-regulated *Luciferase* reporter. (a) Trans-repression of AR-dependent gene expression by FoxA1 from an ARE-containing reporter in transfected PC3-AR cells. **(b)** Co-IP analysis of the interaction of FoxA1 with the full length or truncated AR in transfected HEK293 cells. (**c**) Analysis of an AR mutant panel for potential escape of FoxA1 trans-repression. Nine AR mutants were originally identified in advanced prostate tumors (ref. 41). The trans-repression effect was determined in transfected HEK293 cells in the presence of DHT. Error bars represent standard deviation based on four independent experiments in both *a* and *b*.

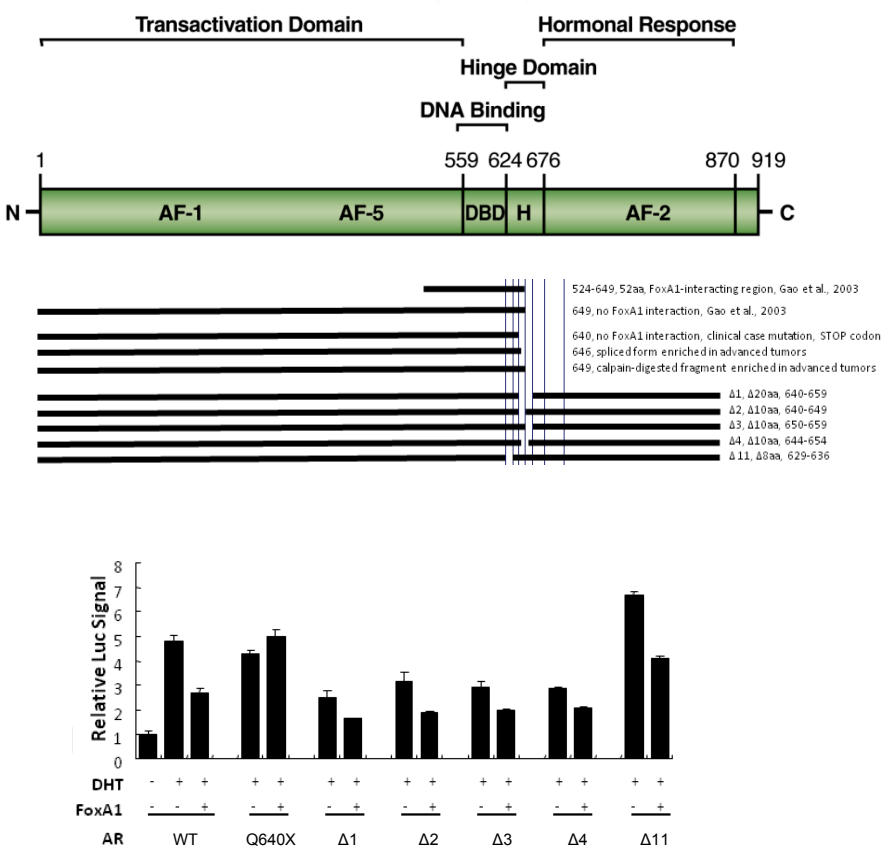

Supplementary Figure 12. AR LBD is involved in FoxA1:AR protein interactions. A series of short deletions were generated affecting the residues located between the 3' end of the Q640X mutant and the 3' end of the reported FoxA1 interacting domain (shown on top). AR deletions were tested by the *Luciferase* assay in HEK293 cells (bottom). Error bars represent standard deviation based on four independent experiments.

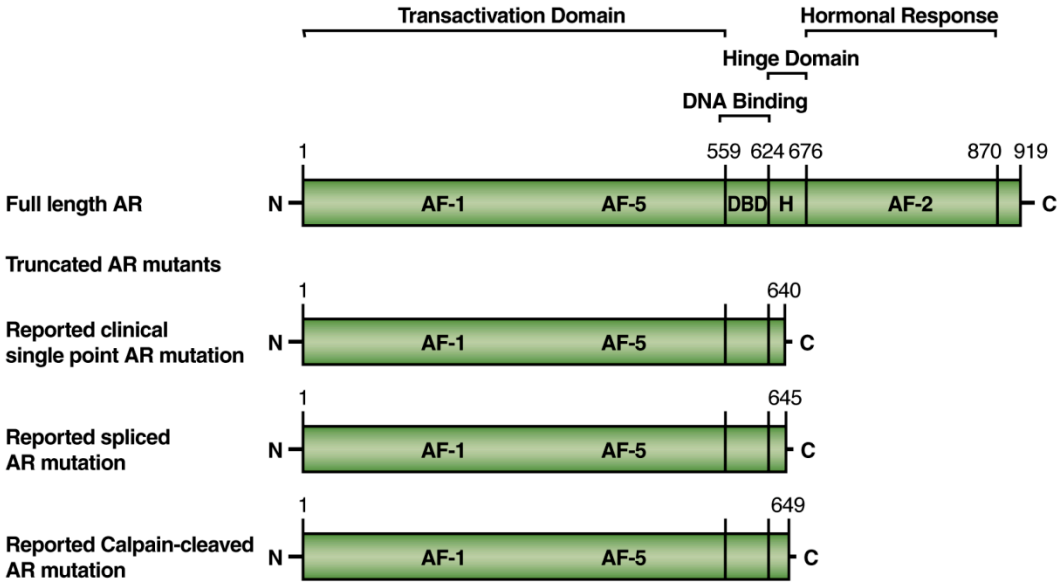

Supplementary Figure 13. Three alternative strategies to generate truncated AR that lacks the ability to bind to FoxA1. Multiple AR abnormalities have been reported in advanced prostate tumors, including a point mutation that creates a stop codon after position 640, frame shift resulting from alternative splicing that causes translation termination at position 645, and calpain-mediated cleavage of AR at position 649, all of which occur in the hinge region critical for FoxA1 interaction with AR.

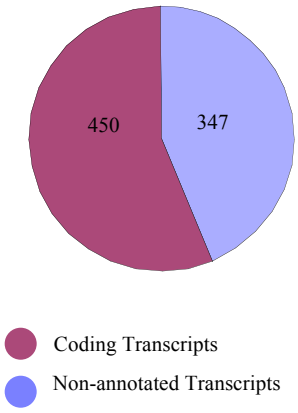

Supplementary Figure 14. DHT-induced coding and non-annotated transcripts identified by GRO-seq. In the DHT induced genes, 450 transcripts are from coding genes and 347 transcripts are non-annotated.

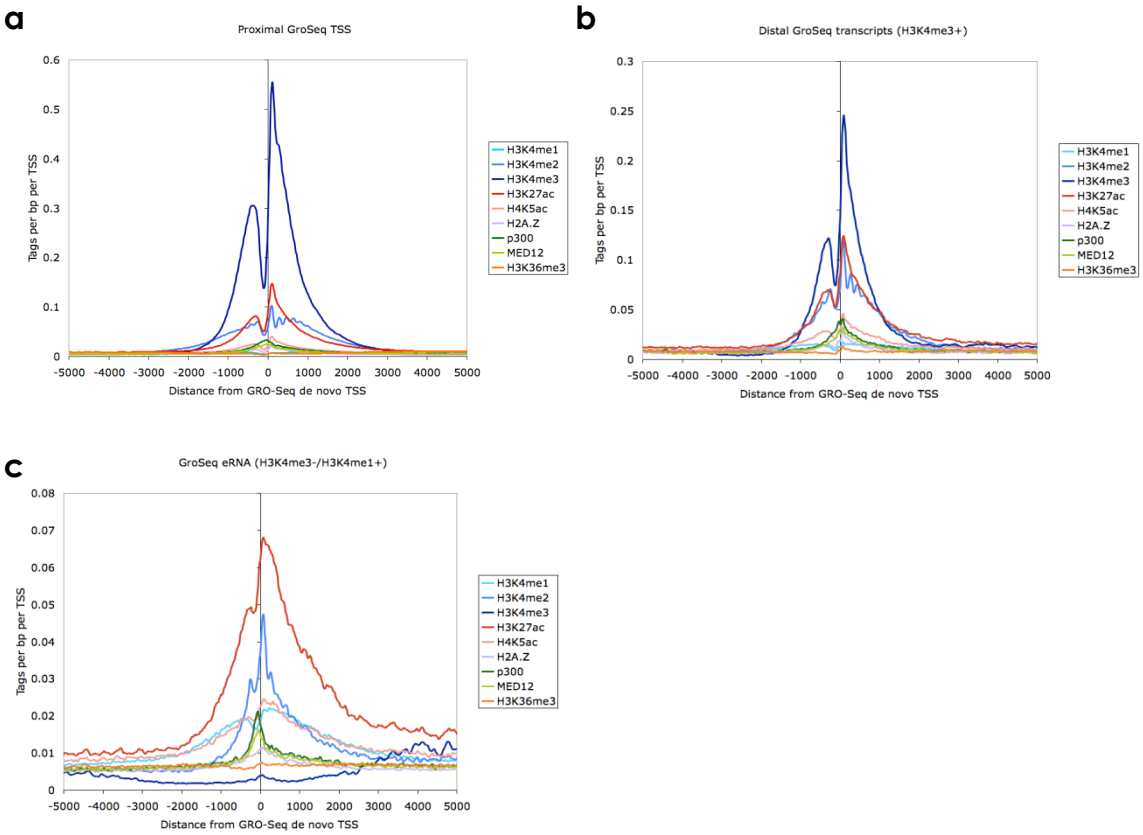

Supplementary Figure 15. Chromatin modifications and architecture at different genomic loci generating eRNA defined by GRO-Seq. **(a)** Normalized ChIP-Seq read density for various histone modifications and co-activators around GRO-seq defined TSSs within 3 kb of RefSeq TSSs **(b)** Same as (a) for GRO-seq defined TSSs around H3K4me3+ regions located > 3kb from RefSeq TSSs. **(c)** Same as (a) for GRO-seq defined TSSs around H3K4me1+/H3K4me3- regions localized >3kb fro RefSeq TSSs.

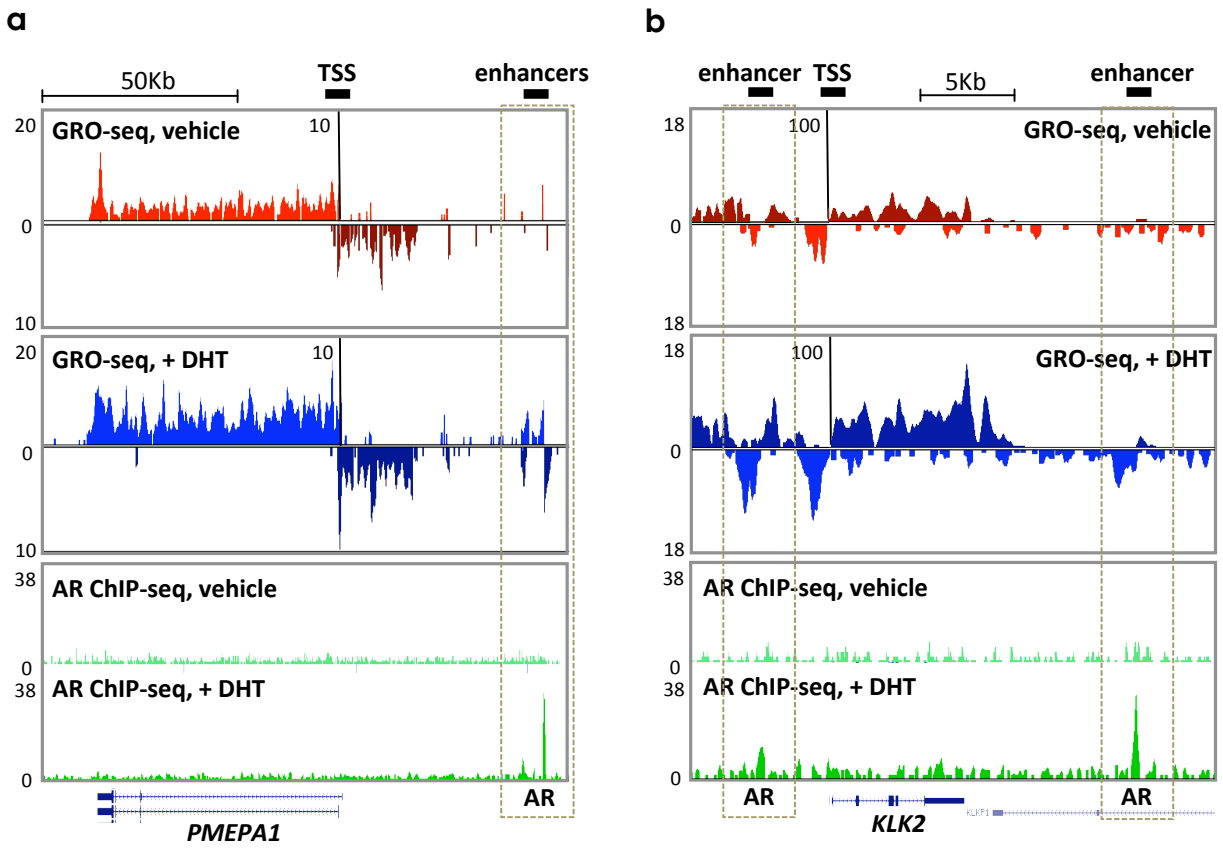

Supplementary Figure 16. Additional illustrative examples of DHT-induced eRNAs. (a, b) Nascent RNA on the classical DHT-regulated *PMEPA1* (*a*) and *KLK2* (*b*) genes. Numbers indicate the scale of normalized read depth. Note different scales for the reads between genic and enhancer regions. The bottom panels show AR binding before and after DHT treatment.

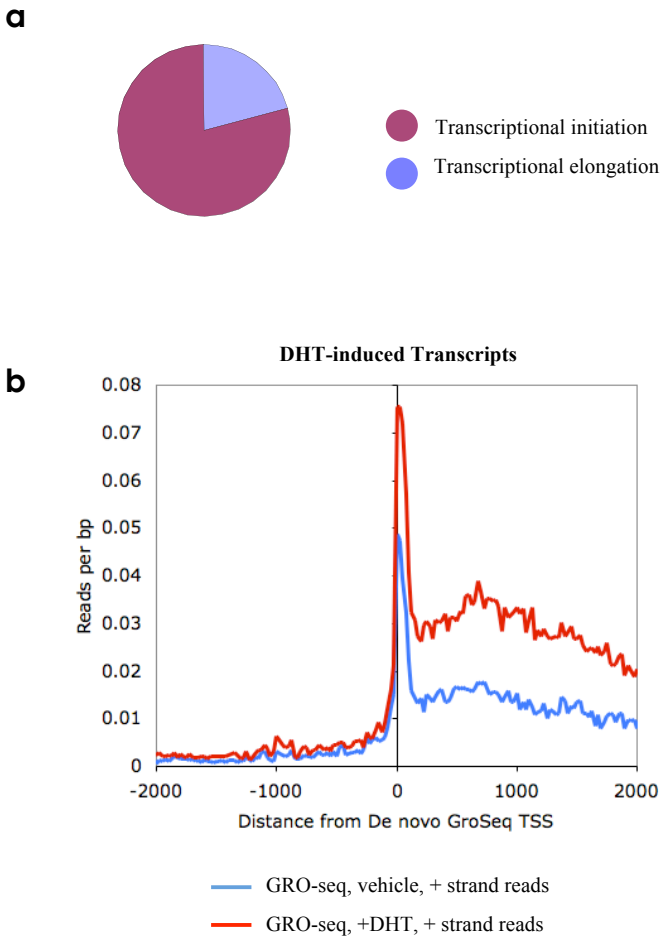

Supplementary Figure 17. The effect of DHT induction on transcriptional initiation or elongation. (a) In the DHT-induced transcripts identified by GRO-seq, 21% showed minimal induction of nascent RNA just downstream of promoter regions (-100 to +200 bp, <1.5 fold) and robust induction of nascent RNA in the gene body (+200 bp to +4000 kb, >1.5 fold), indicating that DHT enhanced transcription elongation on these genes. The remaining transcripts (79%) exhibited a general increase in nascent transcripts throughout the transcribed region, indicating that DHT stimulated transcription initiation from these genes. (**b**) Profile of sense GRO-Seq reads before and after treatment with DHT around the TSS of induced transcripts showing increases in both promoter-associated and gene body nascent RNA.

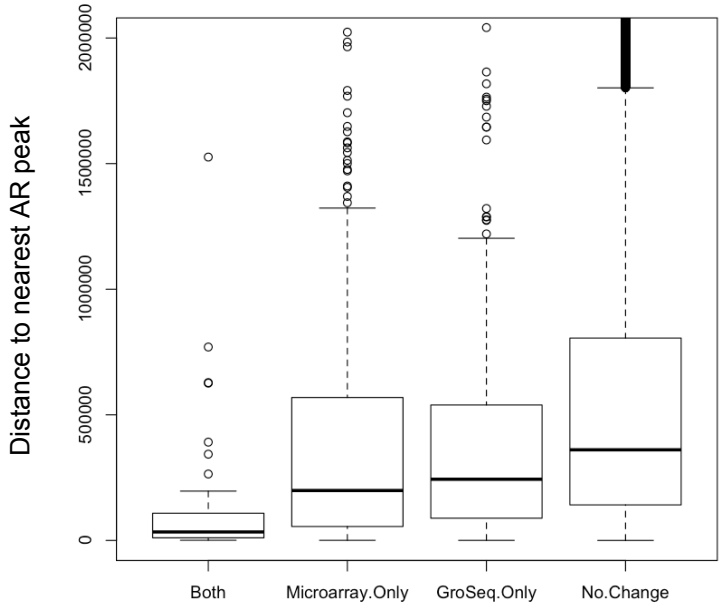

Supplementary Figure 18. Distance to the nearest AR binding sites from DHT-induced genes defined by GRO-seq and/or gene expression arrays. "Both" refers to genes (54) are defined as DHT-induced detected by both GRO-seq (DHT 1h) and microarray (DHT 20h); **"Microarray only"** or **"GRO-seq only"** refer to genes only defined by microarray data (472) or GRO-seq data (301); **"No Change"** means genes not regulated by DHT by either platform, and serves as a negative control.

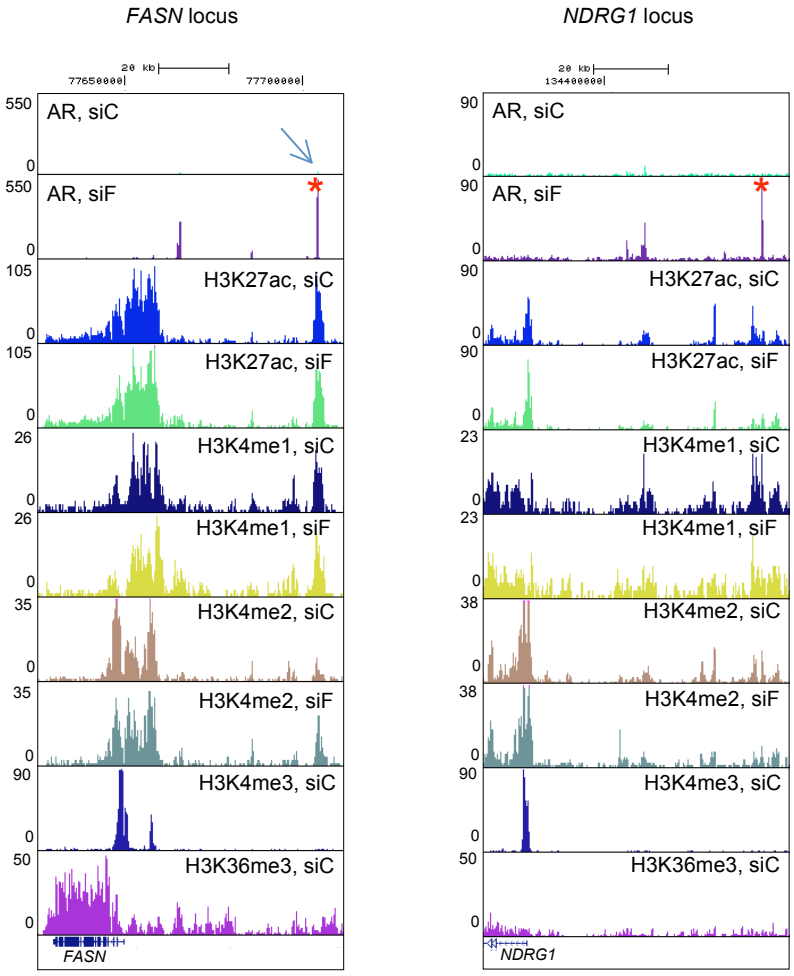

Supplementary Figure 19. Histone marks, AR ChIP-seq profiles around *FASN* and *NDRG1* genes. Multiple enhancer marks are pre-established on the distal AR binding sites induced by *FOXA1* knockdown (red asterisks). All experiments shown were performed in the presence of DHT. The arrow indicates a weak AR binding site detectable by ChIP-seq in control siRNA treated cells (the signal is barely visible because of the scale in the figure). This site is largely induced upon *FOXA1* knockdown.

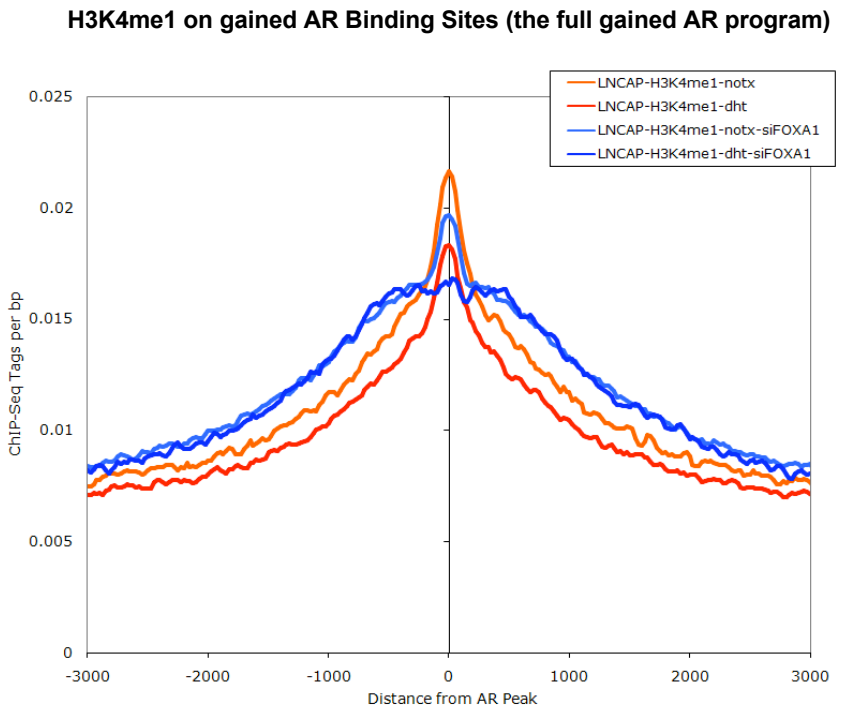

Supplementary Figure 20. Gained AR loci are largely pre-marked with H3K4me1 before *FOXA1* knockdown in LNCaP cancer cells. The data show the similar distribution of H3K4me1 surrounding gained AR loci with or without DHT treatment and before and after *FOXA1* knockdown.

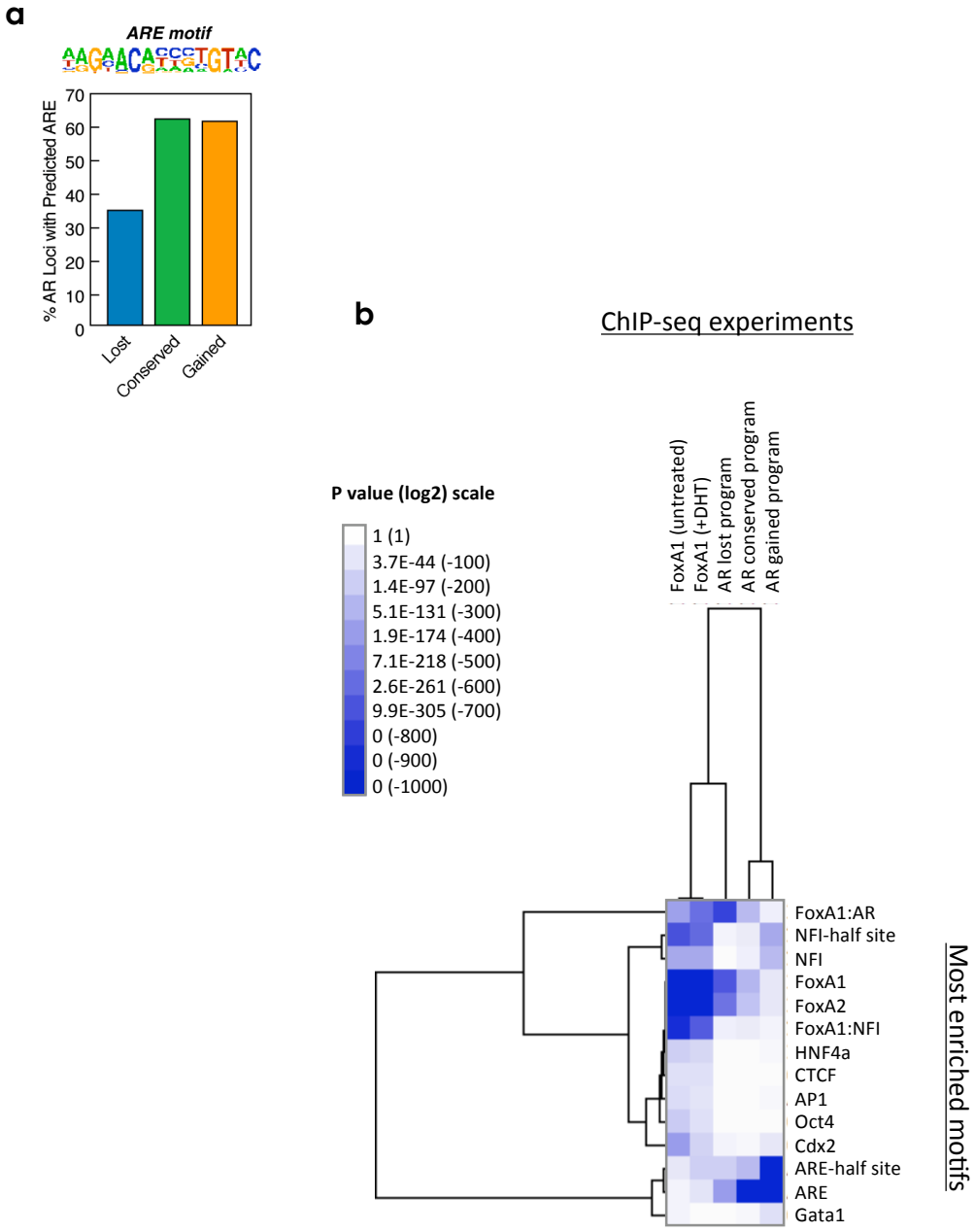

Supplementary Figure 21. Distinct motif patterns are associated with the different AR binding programs observed in LNCaP cells. a) Percentage of AREs present in individual AR programs. (**b**) Hierarchical clustering of motif enrichment revealed that the FoxA1 motif was lost while the NFI and ARE motifs were enriched in the gained AR program.

		Gained Program		Conserved Program		Lost Program	
GO	Term	Rank	P-value	Rank	P-value	Rank	P-value
GO:0008152	metabolic process	1	1.17E-19	5	1.20E-09		0.000479858
GO:0044237	cellular metabolic process	2	1.31E-18	7	1.95E-08	17	7.51E-06
GO:0044249	cellular biosynthetic process	3	1.26E-13	2	1.49E-11		0.005226284
GO:0009058	biosynthetic process	4	1.51E-13	1	3.62E-12		0.008386217
GO:0044238	primary metabolic process	5	2.06E-13	4	8.24E-10		0.000234953
GO:0051186	cofactor metabolic process	6	1.29E-11		0.137658326		1
GO:0006732	coenzyme metabolic process	7	1.44E-09		0.245480125		1
GO:0042254	ribosome biogenesis	8	3.55E-09		0.029564408		0.547401117
GO:0055114	oxidation reduction	9	6.19E-09		0.002187683		0.910637914
GO:0051188	cofactor biosynthetic process	10	1.41E-08		0.371992701		1
GO:0042180	cellular ketone metabolic process	11	1.68E-08		0.002878217		0.452096374
GO:0006082	organic acid metabolic process	12	2.14E-08		0.000517893		0.443005441
GO:0006364	rRNA processing	13	3.05E-08		0.0752835		0.451602836
GO:0019752	carboxylic acid metabolic process	14	6.95E-08		0.002226033		0.436921778
GO:0043436	oxoacid metabolic process	15	6.95E-08		0.002226033		0.436921778
GO:0016072	rRNA metabolic process	16	8.03E-08		0.087225745		0.466426305
GO:0006091	generation of precursor metabolites and ener	17	8.99E-08		0.583534756		0.855219129
GO:0034470	ncRNA processing	18	1.22E-07		0.03751126		0.700472205
GO:0034641	cellular nitrogen compound metabolic process	19	1.91E-07		0.002654963		0.072813465
GO:0034660	ncRNA metabolic process	20	4.26E-07		0.050378031		0.771195271
GO:0006260	DNA replication		0.387204676	3	2.64E-11	2	6.48E-11
GO:0006259	DNA metabolic process		0.802715915	6	4.09E-09	1	1.39E-11
GO:0006261	DNA-dependent DNA replication		0.918809139	8	2.57E-08	4	3.06E-08
GO:0006695	cholesterol biosynthetic process		0.000505785	9	8.78E-08		1
GO:0006807	nitrogen compound metabolic process		3.27E-05	10	3.01E-07		0.000300211
GO:0008610	lipid biosynthetic process		2.18E-06	11	5.69E-07		0.596207955
GO:0006629	lipid metabolic process		2.88E-06	12	7.82E-07		0.739702455
GO:0016126	sterol biosynthetic process		0.000186421	13	1.05E-06		1
GO:0006270	DNA replication initiation		1	14	1.11E-06		0.000129349
GO:0008203	cholesterol metabolic process		0.008465251	15	1.25E-06		1
GO:0006066	alcohol metabolic process		0.001261703	16	1.78E-06		0.702740101
GO:0044255	cellular lipid metabolic process		8.35E-07	17	1.86E-06		0.586610454
GO:0034961	cellular biopolymer biosynthetic process		0.026455255	18	2.69E-06		0.000444515
GO:0016125	sterol metabolic process		0.003337048	19	3.38E-06		1
GO:0043284	biopolymer biosynthetic process		0.019093857	20	3.74E-06		0.000508197
GO:0006268	DNA unwinding during replication		1		0.286467022	3	1.58E-08
GO:0006974	response to DNA damage stimulus		0.980989015		0.01482131	5	6.48E-08
GO:0032508	DNA duplex unwinding		0.773343826		0.356895738	6	7.44E-08
GO:0032392	DNA geometric change		0.773343826		0.356895738	7	7.44E-08
GO:0044260	cellular macromolecule metabolic process		0.000147801		0.002143552	8	9.93E-08
GO:0034984	cellular response to DNA damage stimulus		0.978101301		0.027651409	9	1.46E-07
GO:0007049	cell cycle		0.12380565		0.001979187	10	1.62E-07
GO:0006281	DNA repair		0.97762555		0.018183397	11	1.98E-07
GO:0034960	cellular biopolymer metabolic process		0.000255471		0.002650436	12	3.02E-07
GO:0033554	cellular response to stress		0.825348385		0.044674289	13	2.06E-06
GO:0043170	macromolecule metabolic process		0.001871065		0.011697168	14	5.91E-06
GO:0022403	cell cycle phase		0.02086814		0.006194834	15	6.21E-06
GO:0043283	biopolymer metabolic process		0.003156408		0.011797958	16	6.77E-06
GO:0051716	cellular response to stimulus		0.764453906		0.110368828	18	1.49E-05
GO:0006284	base-excision repair		0.60753604		0.463875052	19	1.89E-05
GO:0000279	M phase		0.034196138		0.00394514	20	3.01E-05

Supplementary Figure 22. Gene Ontology (GO) analysis of the lost, conserved, and gained DHT-responsive gene programs in response to *FOXA1* knockdown. Comparison of the top 20 enriched teams revealed preferential association of the lost program with terms in DNA replication/repair; the conserved program with lipid metabolism and DNA replication, and the gained program with macromolecular biosynthesis and general metabolic processes (cell growth).

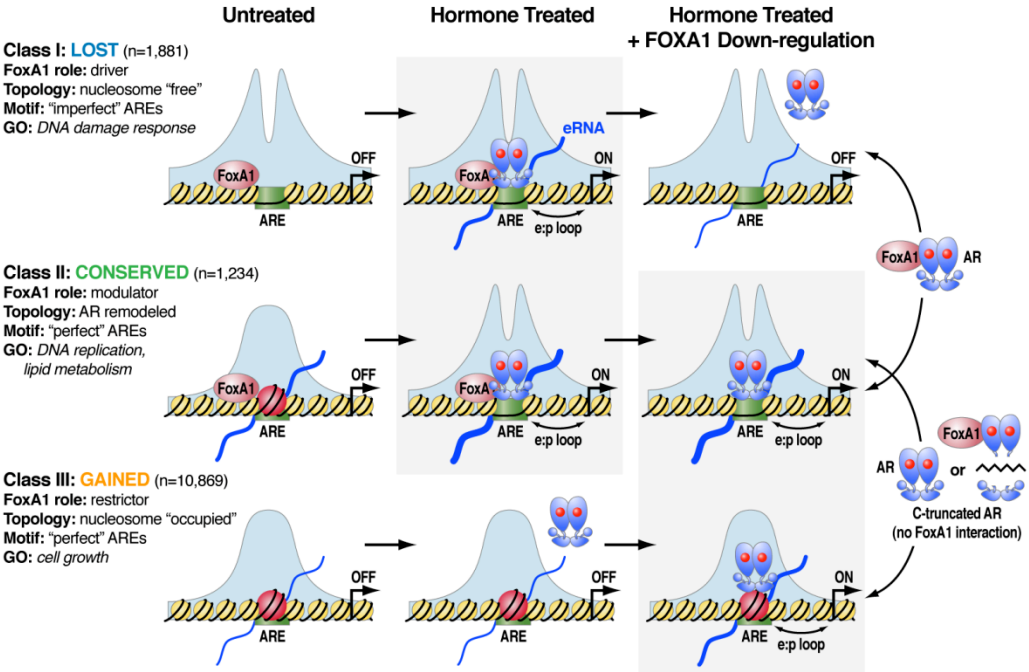

Supplementary Figure 23. Proposed model for FoxA1-mediated AR targeting and reprogramming in LNCaP cells. The model diagrams three classes of AR-bound enhancers and DHT-induced eRNA expression from them. In Class I (lost AR program), FoxA1 pre-occupancy may license AR to bind to those sites upon DHT treatment and to induce eRNAs, a process potentially assisted by direct AR:FoxA1 interactions in addition to their independent DNA binding activities. This lost program in FOXA1 down-regulated cells may enhance genome instability according to GO analysis. In Class II (conserved AR program), AR binds to those sites independent of FoxA1, perhaps due to the presence of canonical AREs, which helps preserve cell proliferation functions. The levels of AR, p300, and Med12 binding as well as eRNA generation are modulated by, but not dependent on, FoxA1. In Class III (gained AR program), FoxA1 normally restricts AR binding and prevents DHT-induced eRNA production, despite the presence of strong AREs. Although pre-established, these gained loci exhibit very unique chromatin organizational features, including a strong central nucleosome, heavily marked by modified histones and the histone variant H2A.Z, none of which is dismissed upon AR binding. AR released from trans-repression by FoxA1 licenses conversion of those sites to androgen-responsive, eRNA-generating enhancers to activate a new androgen-regulated gene expression program, which further facilitates cell proliferation. The FoxA1-mediated AR reprogramming may underlie prostate cancer progression to acquire more aggressive tumor phenotype. The general principle on enhancer switches regulated by cell lineage-specific, signal-induced transcription factors may apply to many other developmental and disease processes.

Primer name	Primer sequence
ARGained1-5	CAGTCTCTGGGACCTCACCT
ARGained1-3	GACAGTGGCAGGTAGGGAAC
ARGained2-5	TGGAGTGCCTATCAGTGCAG
ARGained2-3	ACGGCCAATTACTTGTTTGC
ARGained3-5	TTATCTGATGGCCTCGATCC
ARGained3-3	GCACAGGGTGACTTTGTCCT
ARGained4-5	GACTTCTTGCTGGTGGCTTC
ARGained4-3	GGTTTGCCTTTGTTTCATGG
ARGained5-5	AGGAGTTCTCCAGGCAAACA
ARGained5-3	ACCCAGCCTAACCACAGTGA
ARGained6-5	TGCAGCCTGATCTTCCTCTT
ARGained6-3	TGCTTTGGTCAACAGACTGC
ARGained7-5	TTCGCTGGGTCCAGTATTTC
ARGained7-3	CTGTGTTTCCCAAGCTGACA
ARGained8-5	AGGGCAGCCTCTGAAATCTT
ARGained8-3	GATGCTGCTCATTCAGGTCA
ARGained9-5	ATGGGTCCTGTTTTGTTCCA
ARGained9-3	CGCCAGGCTGATTAAAGAAG
ARGained10-5	ACAAACATTGCCCCATGAGT
ARGained10-3	CTGCCACTGAAGGAGACACA
ARGained11-5	CCTGGACCTGTCCTTTGTGT
ARGained11-3	CAGAGAGCAGAGCAATGCAG
ARGained12-5	CATCTCCACACCCTCACCTT
ARGained12-3	GAGGGAGCAAAACAGTGTCC
ARGained13-5	GATGACCTCGGCCTAATCAA
ARGained13-3	ATCCTGTTCCAGGAGCAATG
ARGained14-5	AGCGTGCTCCTGCCTATTTA
ARGained14-3	CGTAAAGGCAAGGGTGTGAT
ARGained15-5	AAGGACGCTTTCTCTGTCCA
ARGained15-3	TGTGTGCTATGCCCAATGTT
ARGained16-5	TGTCGGTCGCTGAGTTACAG
ARGained16-3	GGACATGACAGGCAGGATCT
ARLost1-5	TGGCAGTTACCGAAAGTGTG
ARLost1-3	TCCAGGTTTTGGGCTATCAC
ARLost2-5	AAATCTGGCTACACGGATGG
ARLost2-3	GGCATGAGAGAACTTTTGCAG
ARLost3-5	GCCACTGTACCTTGGAGAGG
ARLost3-3	AGGAAGGCCATCTGGATTTT
ARLost4-5	TATTGCATTGTCGGGACTTG
ARLost4-3	TAGGGAAGAAAGCTGGCAAC
ARLost5-5	CAGGCAATAGGAAATGTCTGC
ARLost5-3	GTCCCTGAGAACAACCAGGA
ARLost6-5	GCAGGCTGATGCTTCTGTAA
ARLost6-3	AGGCTTTCGTGCCATAAGAA
ARLost7-5	ACCATCATAAGTCTCGGCTTG
ARLost7-3	TCAGTAGGCACTCCCAATCA
ARLost8-5	TGCAAGGTGATGGAAATTCA
ARLost8-3	AGGGTGTCAGGGTGTCAGTC
ARLost9-5	TTCTTCCCTGACCATTTTGG
ARLost9-3	TCAAGGAATGCTCACTGTGG
ARLost10-5	TCACGTAAAGGCATGGTTTG
ARLost10-3	CTTTGGTTCTGTCCCTCTGG
ARLost11-5	GTGTTTGGGCAGAAAAAGGA
ARLost11-3	CATGCAGCGTACTCACAACA
ARLost12-5	ACAATGCCAAGTGTTGGTGA
ARLost12-3	TGGTGGGTGGATTATACCTCA
ARLost13-5	CGTCCCCAGTCACTTTGTTT
ARLost13-3	GTCAAATGCCTTGGAGAGGA
ARLost14-5	GTGAGAGACGGGGAACAAAA
ARLost14-3	TTGAGGCTCTGGGGTTAATG
ARLost15-5	TGTGTAATGGACGGGCAGT
ARLost15-3	TTTTACTGCTCCAGGCTGCT
ARLost16-5	TGTGGTTCAGCTTTGGAAAA
ARLost16-3	CCCTAGGAATGGAATTGCTG
ARLost17-5	AAGCAGACACCCAGAGCCTA

Primer name	Primer sequence
ARLost17-3	TGGTCTCACTTGGTTGACTCC
ARLost18-5	GCCCAGGAGGGAGACTTTAT
ARLost18-3	TTGCATAGCAAACTGCCTTG
ARLost19-5	AACAGCCCCTTTCAAGACTG
ARLost19-3	CATCATCAACAGGAGGGACA
ARLost20-5	GCTTGGCCTGATCATTCACT
ARLost20-3	TGTCATTTCCGAACCCTCTC
ARLost21-5	TGGGAGGACAAGAACAATGA
ARLost21-3	TCCCTGAGCCCTTTCTCTAA
ARLost22-5	CACAGAGGGTCTAGGCATGG
ARLost22-3	GGATCTTTGGCAAGAAGTGTG
ARConserved1-5	TTCCGAAGTGCTGGGATTAC
ARConserved1-3	TACCCATGCAAACACATGCT
ARConserved2-5	TGCCATGTCTGTTTGGGTAA
ARConserved2-3	AGAATCTGGAAAATGGAAGGAA
ARConserved3-5	ACTGGCCCATATTGTTCTGC
ARConserved3-3	TGGGAACAACACCAAACTCA
ARConserved4-5	TCGGCACATTATTGCATTTG
ARConserved4-3	TGCCACATGGTTTTCTTTGA
ARConserved5-5	ACTGTTCAGCAGCACCACAC
ARConserved5-3	ATTGTTGGGTCACTGCTTCC
ARConserved6-5	CACGTGGAAAAACCACTCCT
ARConserved6-3	AGGAGAGCACGTTCCGTAAA
ARConserved7-5	TGGCAAAACAAGCCACATAA
ARConserved7-3	TGCTAGCACCAGTCCCTTTT
ARConserved8-5	GCACCAGGGAACAGACAAAT
ARConserved8-3	AGCCTAATGACCTCCCCTGT
ARConserved9-5	CTGAGGGGAAGTTTGAGTGC
ARConserved9-3	CCCAGGAAGAACAAACCTCA
ARConserved10-5	AACTCTCCAACGTGCCAATC
ARConserved10-3	GCAGTTTATGGCTCCCACAT
ARConserved11-5	GGAACAGCAGGAGGAAAACA
ARConserved11-3	TATACCAGCGTTCCCCAAAG
ARConserved12-5	ACTTAAAGGGGGAGGGAGGT
ARConserved12-3	CAGCTCGCTTGATGTGGTTA
ARConserved13-5	TTGGCAACAGAGTGAGCATC
ARConserved13-3	TTGCACAATTTCCCCTTCTC
ARConserved14-5	CTACTTCTCCCGTGCCACTC
ARConserved14-3	TCTCTCCCCTTCGATGTGTC
ARConserved15-5	TTTTTGGGTCAAGGAAGTGG
ARConserved15-3	GCATCTGCAAGCGATCATAA
ARConserved16-5	GCAGATGAGCAGAAGGGAAG
ARConserved16-3	TCAGCAGAGCCAACACAAAC
ARConserved17-5	TTCCGAAGTGCTGGGATTAC
ARConserved17-3	GGTTGGAACAAAGGGTTCCT
ARConserved18-5	CTCGCCAGTGCTTGTAACCT
ARConserved18-3	CACATGGCAGATGCTCAGTT
ARConserved19-5	AGGGCAACAAAGAACAATGG
ARConserved19-3	AACCTCGACTCTGCTCTGGA
ARConserved20-5	TGGTCAACAAAGCTGGGAAT
ARConserved20-3	GGCTTTCAGCTGATGTCCTC
ARConserved21-5	AGTTCTGCCAGGTGTTCCAC
ARConserved21-3	GGGGGAAAGAGTTGAGAAGC
ARConserved22-5	GACAAAGGAGGAAGCAGCAG
ARConserved22-3	CACTTGCCTGGGAAATATGG
ARConserved23-5	GCTTCAGGTCAAGGTGGTGT
ARConserved23-3	AAACGGGGCAGTAGTTGATG
ARConserved24-5	CCATGGGTAGCCAGTCATCT
ARConserved24-3	AATGCAAAACCATCTCATTGC
ARConserved25-5	CTGGGGCCATTTATTTTCAA
ARConserved25-3	ATGCATACAGGGCTTCGTTC
ARConserved26-5	CACTGAATGGGTGTCACCTG
ARConserved26-3	TTTGAACACACCTGGGAACA
ARConserved27-5	TCTGGCACAGATTGACTTGC
ARConserved27-3	AGTGGAGGCTTAAGGGAGGA

Supplementary Figure 24 Primers used for ChIP-qPCR analysis in this study.

Antibody	Cell Type	siRNA	Treatment	Total Mapped Tags (hg18)	Peaks/ Regions	Peak Finding Parameters [default: peak size = 200 bp, FDR<0.001, >4x over input signal, >4x over local signal]
AR	LNCaP	siCTL	+dht	12,369,597	3,115	
AR	LNCaP	si*FOXA1*	+dht	7,752,382	12,103	
AR	LNCaP	siCTL	+vehicle	12,340,126	205	
FoxA1	LNCaP	siCTL	+vehicle	7,853,276	48,129	
FoxA1	LNCaP	siCTL	+dht	7,879,378	33,426	
H3K4me1	LNCaP	siCTL	+vehicle	7,660,303	45,931	Peak size 2000 bp, >3x input, >1x local
H3K4me1	LNCaP	siCTL	+dht	11,347,500	51,544	Peak size 2000 bp, >3x input, >1x local
H3K4me1	LNCaP	si*FOXA1*	+vehicle	13,993,617	61,405	Peak size 2000 bp, >3x input, >1x local
H3K4me1	LNCaP	si*FOXA1*	+dht	8,711,004	47,586	Peak size 2000 bp, >3x input, >1x local
H3k4me2	LNCaP	siCTL	+vehicle	9,422,758	49,826	Peak size 1000bp, Mnase
H3k4me2	LNCaP	siCTL	+dht	10,186,956	49,308	Peak size 1000bp, Mnase
H3k4me2	LNCaP	si*FOXA1*	+vehicle	9,116,636	44,828	Peak size 1000bp, Mnase
H3k4me2	LNCaP	si*FOXA1*	+dht	7,975,165	42,264	Peak size 1000bp, Mnase
H3K4me3	LNCaP	siCTL	+dht	15,188,174	14,283	Peak size 1000bp
H3K27ac	LNCaP	siCTL	+dht	10,228,155	48,385	Peak size 1000bp
H3K27ac	LNCaP	si*FOXA1*	+dht	9,864,179	45,770	Peak size 1000bp
H4K5ac	LNCaP	siCTL	+dht	9,273,559	54,426	Peak size 2000bp, >3x input, >1x local
H4K5ac	LNCaP	si*FOXA1*	+dht	7,247,434	42,384	Peak size 2000bp, >3x input, >1x local
H3K36me3	LNCaP	siCTL	+dht	9,810,690	52508	
H2AZ	LNCaP	siCTL	+dht	11,711,146	16392	Peak size 2000bp, >3x input, >1x local
H2AZ	LNCaP	si*FOXA1*	+dht	9,355,679	7841	Peak size 2000bp, >3x input, >1x local
p300	LNCaP	siCTL	+dht	4,161,562	4295	
p300	LNCaP	si*FOXA1*	+dht	3,871,540	5730	
MED12	LNCaP	siCTL	+dht	5,260,539	3365	
MED12	LNCaP	si*FOXA1*	+dht	5,332,366	5618	
GRO-seq	LNCaP	siCTL	+vehicle	10,084,264	-	
GRO-seq	LNCaP	siCTL	+dht	11,943,507	-	
GRO-seq	LNCaP	si*FOXA1*	+dht	10,611,010	-	
Input	LNCaP	-	-	44,140,163	-	

Supplementary Figure 25. Summary of ChIP-seq experiments performed in this study. ChIP-seq analysis in DHT and mock treated (1hr or 4hrs for MNases-treated experiments) combined with *CTL* or *FOXA1* siRNA treatment in LNCaP cells. Peak analysis was performed as described in Supplementary information.